Foot and Ankle Surgery 30 (2024) 7–20

Contents lists available at ScienceDirect

Foot and Ankle Surgery

journal homepage: www.journals.elsevier.com/foot-and-ankle-surgery

Diagnostic applications and benefits of weightbearing CT in the foot and ankle: A systematic review of clinical studies

Jing Li [a,1], Mengze Fang [a,1], Aline Van Oevelen [a], Matthias Peiffer [a], Emmanuel Audenaert [a], Arne Burssens [a,*], International Weightbearing CT Society [b]

[a] *Department of Orthopaedics, Ghent University Hospital, Ghent, Belgium*
[b] *International Weightbearing CT Society: Martinus Richter, François Lintz, Cesar de Cesar Netto, Scott J Ellis, Alexandre Leme Godoy-Santos, Alessio Bernasconi, Arne Burssens, Ghent, Belgium*

A R T I C L E I N F O

Article history:
Received 28 May 2023
Received in revised form 16 August 2023
Accepted 1 September 2023

Keywords:
Weightbearing CT (WBCT)
Ankle osteoarthritis
Hindfoot deformity
Midfoot instability
Forefoot alignment

A B S T R A C T

Background: Foot and ankle weightbearing CT (WBCT) imaging has emerged over the past decade. However, a systematic review of diagnostic applications has not been conducted so far.
Method: A systematic literature search was performed according to the Preferred Reporting Items for Systematic Reviews and Meta-Analysis (PRISMA) guidelines after Prospective Register of Systematic Reviews (PROSPERO) registration. Studies analyzing diagnostic applications of WBCT were included. Main exclusion criteria were: cadaveric specimens and simulated WBCT. The Methodological Index for Non-Randomized Studies (MINORS) was used for quality assessment.
Results: A total of 78 studies were eligible for review. Diagnostic applications were identified in following anatomical area's: ankle (n = 14); hindfoot (n = 41); midfoot (n = 4); forefoot (n = 19). Diagnostic applications that could not be used on weightbearing radiographs (WBRX) were reported in 56/78 studies. The mean MINORS was 9.8/24 (range: 8–12).
Conclusion: Diagnostic applications of WBCT were most frequent in the hindfoot, but other areas are on the rise. Post-processing of images was the main benefit compared to WBRX based on a moderate quality of the identified studies.

Contents

1. Introduction

Weightbearing radiographs (WBRX) are widely used for the diagnosis and outcome assessment of patients with foot and ankle disorders [1,2]. Despite their ubiquity, plane radiographs contain

* Correspondence to: Department of Orthopaedics and Traumatology, Ghent University Hospital, Corneel Heymanslaan 10, 9000 Ghent, OVL, Belgium.
E-mail address: Arne.Burssens@uzgent.be (A. Burssens).
[1] These authors contributed equally to this manuscript

https://doi.org/10.1016/j.fas.2023.09.001
1268-7731/

several significant shortcomings; accurate analysis is impeded by the superposition of the osseous structures, differences in patient positioning cause measurement errors, and the result is a two-dimensional (2D) projection of a three-dimensional (3D) structure [3]. Computed tomography (CT) imaging technology is commonly used to evaluate skeletal disorders and is able to overcome the shortcomings of superposition by allowing circumferential imaging of the osseous structures and correction of rotational errors by a post-imaging reconstruction of the foot position [4]. However, one major drawback of conventional CT has been the inability to obtain weightbearing images [5]. The importance of weightbearing during foot and ankle radiographic imaging is reflected in different studies, which demonstrated an underestimation of deformity in absence of weightbearing [1,6].

Over the past decade, technological advances allowed to merge the benefits of weightbearing with those of cone-beam CT devices. This resulted in the genesis of weightbearing CT (WBCT) devices that are currently used in clinical practice. Moreover, these WBCT devices continue to evolve with mobile and flexible gantries that allow expansion of WBCT from the foot and ankle up to the knee and hips [7,8]. Additional benefits from this imaging modality include a fast image acquisition time, a compact design, a reduced cost, and radiation dose [8,85]. The introduction of WBCT has permitted the collection of detailed foot and ankle imaging obtained in a standing position [7]. However, WBCT is currently not yet widely used, the specific diagnostic applications are scattered across the literature and the potential benefits are not well assessed in a comprehensive overview [9]. Therefore, we performed a systematic literature search of the diagnostic landscape that can benefit from WBCT imaging in the foot and ankle. We aim to identify several disorders per anatomical area in the foot and ankle that present benefits of WBCT after a decade of research in the field of WBCT imaging.

2. Methods

The Database of Abstracts of Reviews of Effects (DARE), the Cochrane Database of Systematic Reviews (CDSR), and the International Prospective Register of Systematic Reviews (PROSPERO) could not identify previously performed systematic reviews on WBCT of the foot and ankle. The original protocol for this study was registered on PROSPERO, the international prospective register of systematic reviews, which can be accessed online (CRD42022382037). The literature was systematically reviewed according to the Preferred Reporting Items for Systematic Reviews and Meta-Analysis (PRISMA) guidelines. The searched electronic databases included PubMed, Cochrane Library, Embase, and Web of Science. Studies assessing the relationship between WBCT and ankle, hindfoot, midfoot, and forefoot were identified. For every database, the same search strategy was repeatedly performed, combining the following search terms: "weightbearing/standing CT/CBCT and ankle", "weightbearing/standing CT/CBCT and hindfoot", "weightbearing/standing CT/CBCT and midfoot", "weightbearing/standing CT/CBCT and forefoot". A data search was performed from inception until December 2022. The results of this search were evaluated in two steps, by first screening the abstracts and second reading the full text. The in- and exclusion criteria were assessed by two coauthors (JL, MF). Studies were excluded if they reported cadaveric samples, described healthy subjects, were case reports, studied fewer than 15 patients, or were published before 2010. The lead author (JL; board certified orthopaedic surgeon) screened titles and abstracts and selected studies for review. Two coauthors (AVO, MP; orthopaedic PhD researchers) discussed the results to secure that abstracts were not unnecessarily excluded. The full text of these studies was evaluated by two coauthors (JL, MF). Selected studies for retrieval and evaluation were divided into four groups: WBCT and ankle, WBCT and hindfoot, WBCT and midfoot, and WBCT and forefoot. Clinical and radiological data and methods were assessed for each group. Additionally, the study's type and source of funding were recorded. A meta-analysis was initially planned to complement the systematic narrative review. However, this was hampered by the significant heterogeneity in study design and results. Therefore, this synthesis was conducted to explore findings within and between studies, guided by the PRISMA guidelines. Quality assessment of both comparative and non-comparative studies was performed relying on the Methodological Index for Non-Randomized Studies (MINORS) criteria. As reported by Slim et al. [88], the checklist covered the following eight categories to assess non-randomized controlled trials (NRCTs): clearly stated objectives, the inclusion of consecutive subjects, prospective collection of data, appropriate endpoints, unbiased assessment of the study endpoints, a follow-up period in line with study objectives, loss to follow-up less than 5% and a prospective sample size calculation. Each of these questions can be answered with "not indicated" (0 points), "indicated but insufficient" (1 point), or "indicated and sufficient" (2 points), the global ideal score being 16 for non-comparative studies. Two reviewers assessed the MINORS checklist separately for each study (JL, AB). Differences were resolved by a debate with a third independent reviewer (EA; board certified orthopaedic surgeon) lacking standardized evidence, categorization of the MINORS scores was performed based on the study by Ekhtiari et al. [89]: "Very low"(0–4 points); "Low"(5–8 points); "Good"(9–12); and "Excellent"(13–16).

3. Results

A total of 522 studies were included following an electronic database search and screening of the reference lists. Studies were excluded for being duplicates (n = 350), review studies (n = 8), reports not retrieved (n = 3), and reports excluded (n = 83). As a result, 78 studies were confirmed eligible for review (Fig. 1). These consist of 11 prospective studies, 65 retrospective studies, and 2 diagnostic studies. The median sample volume of patients included in the studies was 30 (range: 16–4987). The mean MINORS of the 78 studies was 9.8 on a total of 24 (The global ideal score being 16 for non-comparative studies and 24 for comparative studies). There are 7 level II evidence studies, 68 are level III evidence, and 3 level IV evidence studies. A total of 35 studies described that their work was done without financial support, 19 studies reported industry funding and 24 studies did not report funding. Definition of alignment, evaluation of joint width and spatial interpretability of images in 3D were identified as the main benefits compared to WBRX (Table 5).

3.1. Ankle

A total of fourteen studies [10–23] addressed disorders at the ankle joint (Table 1). Seven studies [10–16] focused on ankle osteoarthritis. In ankle osteoarthritis studies using 2D measurement variables, WBCT mainly concentrated on quantifying the tibiotalar [10,11,13,15] and subtalar [12,14,16] joint alignment. Kim et al. [13,15] used WBCT to assess the internal rotation of the talus in the axial plane in patients with varus ankle osteoarthritis. Kang et al. [14] analyzed the talar tilt, subtalar inclination angle, and calcaneal inclination angle to evaluate the orientation of the calcaneus relative to the talus in the varus ankle osteoarthritis. Hintermann et al. [11] measured the lateral distal tibial angle in the sagittal plane and coronal plane to assess axial rotation between the talus and tibia in total ankle arthroplasty. Krähenbühl et al. [12,16] used WBCT to analyze the tibiotalar angle, subtalar vertical angle, and the medial distal tibial angle. In addition, they reported that the subtalar joint orientation might be a risk factor for the progression of ankle joint osteoarthritis [12,16].

Seven studies [17–23] focused on the diagnostic applications of WBCT in ankle syndesmotic injuries. In studies using 2D

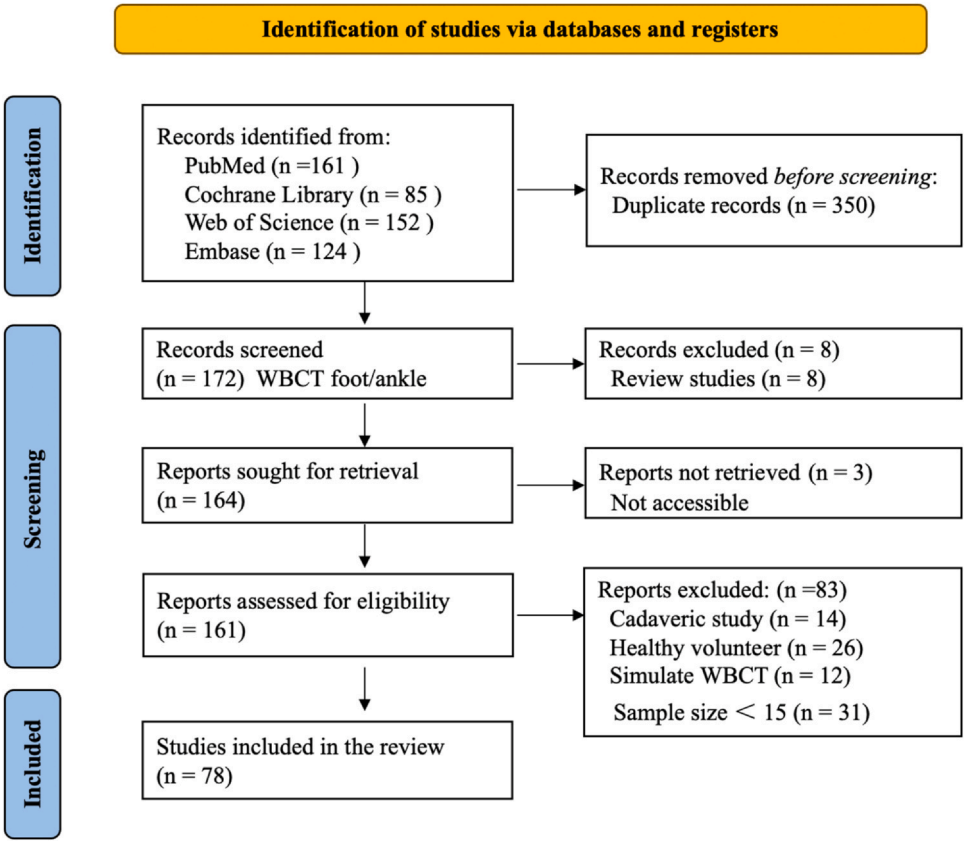

Fig. 1. Flowchart according to the Preferred Reporting Items for Systematic Reviews and Meta-Analysis (PRISMA) guidelines.

measurement variables of ankle syndesmosis, Goldberg et al. [19] analyzed the position of the fibula in the axial plane for patients with syndesmotic injuries. They found weightbearing results in lateral and posterior translation and external rotation of the fibula about the incisura. Three studies [17,22,23] reported that WBCT improved the evaluation of joint width. Patel et al. [17] analysed the relationship between the fibula and tibia for translation and rotation for patients with syndesmotic injuries. Rio et al. [22] used WBCT to evaluate the syndesmotic diastasis area for patients after acute injury. Rooney et al. [23] assessed the reliability of measurement techniques for syndesmosis position after operative fixation of distal tibia platfond fracture on WBCT. Their study reported that WBCT demonstrated significantly greater diastasis in unstable ankles than conventional CT. In studies using 3D measurement variables (Figs. 2, 3), three studies [18,20,21] reported that WBCT scans were an excellent method for 3D reconstruction to improve spatial interpretability. Peiffer et al. [18] used 3D measurement variables and statistical shape modelling to facilitate the diagnostic workup of syndesmosis ankle lesions under weightbearing conditions. Esfahani et al. [20] created 3D models using volumetric measurements up to 5 cm above the tibial platfond and showed higher sensitivity and specificity for recognizing an unstable syndesmosis; Shakoor et al. [21] took measurements 5 mm below the talar dome evaluating the lateral clear space and the medial clear space.

3.2. Hindfoot

A total of 41 studies [24–64] focused on the diagnostic applications located at the hindfoot (Table 2). In studies using 2D measurement variables of the hindfoot, WBCT mainly focused on improving the definition of alignment [26,27,31,35,39,42,49] and improving the evaluation of joint width [43,45–47,50]. Hirschmann et al. [27] measured the hindfoot alignment angle and tibiocalcaneal distance and found that alignment of the hindfoot significantly changes in weightbearing position. Bakshi et al. [31] measured the calcaneal moment arm and found that the hindfoot valgus was associated with first metatarsal (M1) pronation, and the hindfoot varus was associated with M1 supination. Fuller et al. [42] used WBCT to evaluate medial arch anatomy. Six studies [45–50] have also used WBCT to assess various aspects of hindfoot anatomy and diagnose specific conditions. More specifically, de Cesar Netto et al. [45] used WBCT to observe peritalar subluxation in patients with progressive collapsing foot deformity (PCDF) and evaluated the correlation between WBCT markers of peritalar subluxation and Magnetic Resonance Imaging (MRI) [47]. Findings of soft tissue insufficiency in patients with PCFD, corresponded with WBCT markers of pronounced deformity and peritalar subluxation were significantly correlated to MRI involvement of the posterior tibial tendon; Lalevée et al. [46] used WBCT to measure the peritalar subluxation and foot and ankle offset (FAO) to evaluate lateral bony impingements; Kim et al. [49] and Jeng et al. [50] used WBCT to measure the talocalcaneal and calcaneofibular distance to diagnose calcaneofibular impingement.

In studies [25,28–30,32–34,36–38,40,41,44,48,51–64] using 3D measurement variables of the hindfoot,Burssens et al. [25,28,33,34] translated routine radiographic 2D hindfoot measurements towards their 3D equivalents based on segmentation of the CT- slices (Fig. 2). Afterwards, these 3D measurements were used to assess the outcome of the hindfoot alignment (HA) after infra- and supra malleolar osteotomies [25,34]. Peiffer et al. [32] measured the calcaneal osteotomy angle in 3D variables to assess the correlation between the pre-operative hindfoot valgus deformity and calcaneal osteotomy

Table 1
Literature review of ankle studies.

Study	Subjects	Diagnostic applications	Potential benefits	Findings	Level of evidence
Ankle disorders					
Ankle Osteoarthritis					
Willey et al.,[10]	P (n = 20)	Quantified joint-space after tibial-pilon fracture.	Improved evaluation of joint space width.	The mean tibiotalar joint space was 21% less in the injured ankles compared with uninjured ankles.	Prospective Level III
Hintermann et al.,[11]	P (n = 48)	Assessed the relative axial rotation between the talar and tibial of total ankle arthroplasty components per- and postoperative.	Improved quantification of rotation.	The mean intra- and postoperative axial talar component positions were 1.7° (14 internal to 14 external) and 1.4° (12 internal to 20 external).	Retrospective Level III
Krähenbühl et al.,[12]	P (n = 60) HI (n = 20)	Determined the orientation of the subtalar joint in ankle osteoarthritis.	Improved definition of alignment.	Varus osteoarthritis of the ankle joint occurred with varus orientation of the subtalar joint; In patients with valgus osteoarthritis, valgus orientation of the subtalar joint was found.	Retrospective Level III
Kim, et al.,[13]	P (n = 96) HI (n = 52)	Assessed the internal rotation of the talus in varus ankle osteoarthritis.	Improved quantification of rotation.	The incidence of abnormal internal rotation of the talus was 45%.	Retrospective Level III
Kang et al.,[14]	P (n = 100)	Orientation of the calcaneus relative to the talus in ankle osteoarthritis.	Improved definition of alignment.	The position of the calcaneus appears compensatory with coronal plane orientation in varus ankle osteoarthritis when the talar tilt is ≤ 9.5°.	Retrospective Level IV
Kim et al.,[15]	P (n = 102) HI (n = 38)	Alignment of the ankle in medial gutter arthritis.	Improved evaluation joint space width.	The mechanical axis of the lower extremity and the tibial plafond were varus angulated, and the talus was medially translated.	Retrospective Level IV
Krähenbühl et al.,[16]	P (n = 88) HI (n = 27)	Subtalar joint alignment in different stages of ankle osteoarthritis.	Improved definition of alignment.	Varus ankles compensate in the subtalar joint for deformities above the ankle joint. Compensation does not correlate with the stage of ankle osteoarthritis.	Retrospective Level III
Syndesmotic Ankle Injuries					
Patel et al,[17]	P (n = 100)	Analyzed the translation between the fibula and tibia in patients with tibiofibular syndesmosis.	Improved evaluation of joint space width.	The upper limit of lateral translation in uninjured patients was 5.27 mm, and anteroposterior translation lay within the ranges 0.31–2.59 mm and −1.48–3.44 mm, respectively. Higher than this may be indicative of syndesmotic injury.	Retrospective Level III
Peiffer et al.,[18]	P (n = 26) HI (n = 38)	Statistical shape model-based tibiofibular assessment of syndesmotic ankle.	Improved spatial interpretability, the definition of alignment.	Statistical shape modeling combined with patient specific ligament wrapping techniques can facilitate the diagnostic workup of syndesmosis ankle lesions under weightbearing conditions.	Retrospective Level III
Malhotra et al.,[19]	P (n = 26)	Measured the translation and rotation in the axial plane of the fibula.	Improved quantification of rotation.	Weightbearing results in lateral and posterior translation, and external rotation of the fibula in relation to the incisura.	Retrospective Level III
Ashkani et al.,[20]	P (n = 24) HI (n = 24)	Measured the 3D volume of the distal tibiofibular space with syndesmotic instability.	Improved spatial interpretability, and area and volume measurements.	3D volume measured from the tibial plafond to a level 5 cm proximally, where a sensitivity of 95.8%, a specificity of 83.3%, and an accuracy of 90% are reached.	Retrospective Level III
Shakoor et al.,[21]	P (n = 27)	Compared twelve standardized syndesmoses at two axial planes between weightbearing and non-weightbearing modes.	Improved spatial interpretability and joint space width evaluation.	Mean values of the medial clear space on weightbearing images were significantly lower than on non-weightbearing images measurements. No significant difference between the remaining weightbearing and non-weightbearing measurements.	Retrospective Level III
Rio et al.,[22]	P (n = 39)	Evaluated the dynamic change in area with syndesmotic injuries in non-weightbearing and weightbearing positions.	Improved evaluation of joint space width.	Non-weightbearing compared to weightbearing in unstable ankle (13.7% [16.6 ± 9.9 mm2]) versus uninjured ankleS (3.1% [3.4 ± 6.7 mm2]).	Prospective Level III
Rooney et al.,[23]	P (n = 26)	Evaluated reliability of measurement techniques for syndesmosis position after operative fixation of distal tibia plafond fracture.	Improved evaluation of joint space width.	The Nault technique demonstrated moderate-to-excellent interrater reliability (ICCs: 0.67–0.98), apart from the angle of rotation measurement (ICCs: 0.18–0.67).	Prospective Level III

Abbreviations: P, patients; HI, healthy individuals; 3D, three dimensional; ICC, intra class correlation coefficient.

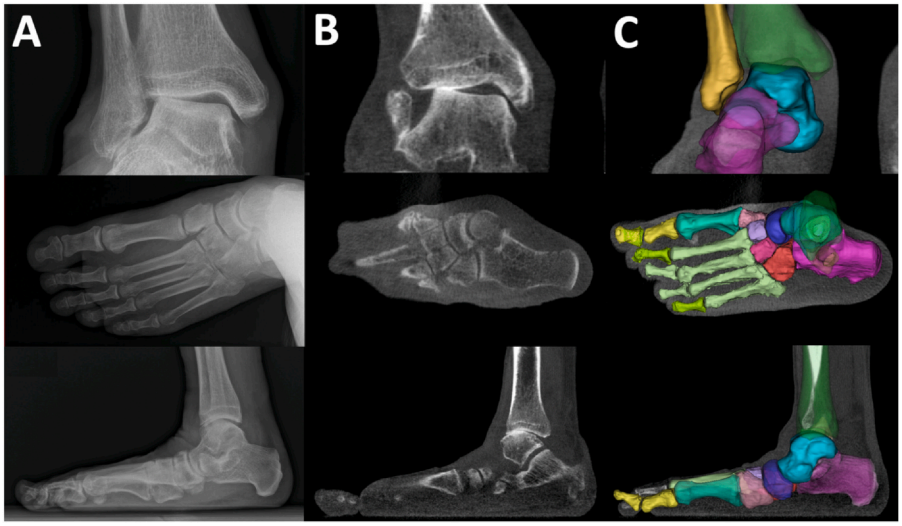

Fig. 2. Patient with progressive collapsing foot deformity (PCFD) assessed by (A) weightbearing radiographs using an anterior-posterior, dorsal-plantar and lateral view (B) weightbearing CT (WBCT) imaging after 2D reconstruction in the frontal, axial and lateral view (C) WBCT imaging after 3D reconstruction using in Mimics® (Materialise, Haasrode, BE) in the frontal, axial and lateral view.

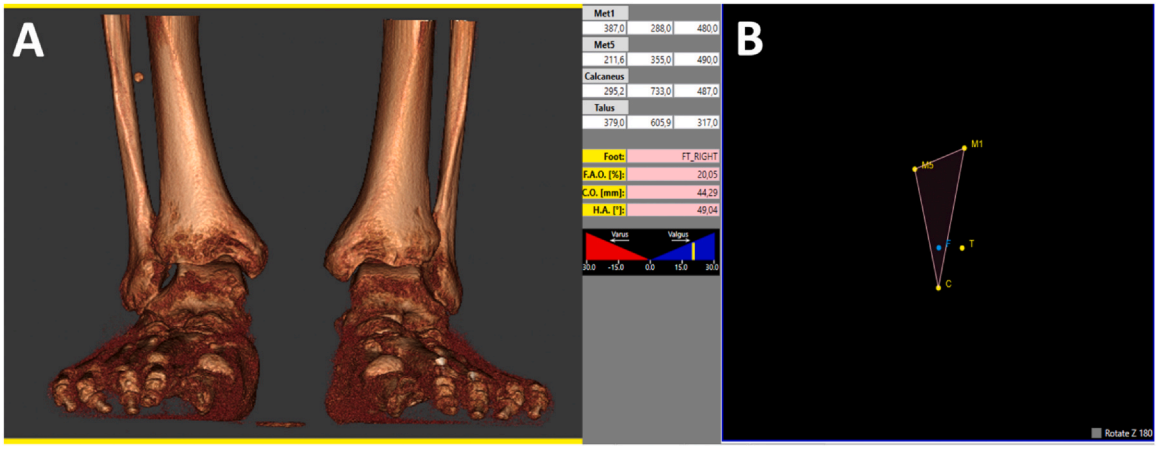

Fig. 3. Explanation of the foot and ankle offset (FAO) A. Three-dimensional model of the previous patient with PCFD B The FAO determined the hindfoot axis relative to the ankle and base of the first as well as the fifth metatarsal head using the foot ankle offset on WBCT datasets. Hereby, a marked planovalgus deformity is observed on the scale bar.

angles and the post-operative calcaneal displacement. Bernasconi et al. [26] and de Cesar Netto et al. [37] measured HA in the national football league and the national basketball association players. They found that WBCT can provide valuable information about anatomic risk factors for common injuries in professional players. de Cesar Netto et al. [51,52,54,58] measured hindfoot and midfoot angles in PCFD and reported that weightbearing 3D images improved the spatial interpretability of articular incongruency compared with traditional CT images. Lintz et al. [29,36] determined the hindfoot axis relative to the ankle and base of the first as well as the fifth metatarsal head using the foot ankle offset (FAO) on WBCT datasets (Fig. 3). Hereby, a 3D perspective is given with excellent intra- and interobserver reliability. Moreover, the FAO has been utilized as a valid tool in patients with ankle instability, total ankle replacement and pre- versus post-op comparisons [29,35,36,90]**.** Day et al. [41] measured the subtalar joint space width following intra-articular calcaneal fractures; Bernasconi et al. [38] quantified hindfoot angles using 3D measurements; Krähenbühl et al. [48] used 3D measurement to diagnose sinus tarsi impingement; Day et al. [55] evaluated PCDF using both 2D and 3D imaging techniques in standing position; Behrens et al. [56] used 3D coverage mapping techniques to evaluate the talonavicular and calcaneocuboid interfaces; An et al. [63] used 3D WBCT analysis to isolate and quantify the multiplanar rotational deformation of the talonavicular joint in patients with Charcot-Marie-Tooth disease. Their studies [29,36,38,41,48,55,56,63] reported that multi-planar weightbearing imaging obtained from WBCT has excellent intra- and inter-observer reliability in assessing alignment and aids surgeons in deciding the appropriate treatment strategy (e.g. osteotomies vs realignment arthrodesis).

3.3. Midfoot

A total of four studies [65–68] addressed disorders at the midfoot (Table 3). Two studies focus on Lisfranc injuries, Sripanich et al. [65] and Falcon et al. [66] used 2D variables to measure the distance between the medial cuneiform and second metatarsal to diagnose injuries of the Lisfranc ligamentous complex and evaluate potential subtle injuries. In contrast, Bhimani et al. [67] used 3D variables to measure the volume of the injured Lisfranc joint complex. They reported that WBCT scans can effectively differentiate between stable and unstable Lisfranc injuries [65–67]. Steadman et al. [68] retrospectively reviewed 302 patients to analyze the naviculocuneiform

Table 2
Literature review of hindfoot studies.

Study	Subjects	Diagnostic applications	Potential benefits	Findings	Level of evidence
Hindfoot disorders					
Hindfoot Deformity					
Burssens et al.,[25]	P (n = 29)	Alignment of the hindfoot deformity before and after supramalleolar osteotomy.	Improved spatial interpretability and definition of alignment	The preoperative alignment (tibial anterior surface = 88 ± 4°, tibiotalar surface=82 ± 7°, talar tilt = 5.8 ± 4.9°) relative to postoperative alignment (tibial anterior surface = 93 ± 5°, tibiotalar surface = 88 ± 7°, talar tilt = 4.2 ± 4.5°).	Retrospective Level III
Bernasconi et al.,[26]	P (n = 36) HI (n = 20)	Alignment of the foot in professional athletes.	Improved definition of alignment.	Medial longitudinal arch angle (15° vs 18.3°); Navicular (38.2 mm vs 42.2 mm); Medial cuneiform (27 mm vs 31.3 mm) compared to normal people.	Retrospective Level III
Hirschmann et al.,[27]	P (n = 22)	Alignment of the hindfoot between WBCT and NWBCT.	Improved definition of alignment.	Significant differences were found for all measurements except the hindfoot alignment angle and talocalcaneal distance.	Retrospective Level III
Burssens et al.,[28]	P (n = 48)	Measured 2D hindfoot alignment and 3D hindfoot alignment for patients.	Improved spatial interpretability and definition of alignment.	The mean 2D hindfoot alignment was 0.79° of valgus ± 3.2° and the 3D hindfoot alignment was 8.08° of valgus ± 6.5°.	Retrospective Level III
Lintz et al.,[29]	P (n = 125)	Assessed hindfoot alignment and predicted the risk of associated pathologies by the FAO in patients.	Improved spatial interpretability and definition of alignment.	Patients with FAO between −1.64% and 2.71% had the least risk of degenerative foot and ankle pathology.	Diagnostic study Level II
Arena et al.,[30]	P (n = 375)	Measured the calcaneal moment arm by hindfoot alignment view radiographs and WBCT.	Improved spatial interpretability and definition of alignment.	Hindfoot alignment view radiographs exhibited a mean calcaneal moment arm difference of 3.9 mm in the varus direction compared with WBCT (95% CI, −4.9–12.8).	Retrospective Level III
Bakshi et al.,[31]	P (n = 196)	Analyzed the relation between hindfoot alignment and M1 axial rotation.	Improved definition of alignment.	Hindfoot valgus was related to first metatarsal pronation; Hindfoot varus was related to M1 supination.	Retrospective Level III
Peiffer et al.,[32]	P (n = 16)	Measured the hindfoot valgus and calcaneal displacement pre-and post-operative.	Improved spatial interpretability, novel 3D measurements, and definition of alignment.	The hindfoot valgus changed from 13.1° (± 4.6) pre-operatively to 5.7° (± 4.3) post-operatively. Mean inferior displacement of 3.2 mm (± 1.3) was observed along the osteotomy with a mean inclination of 54.6° (± 5.6), 80.5° (± 10.7), − 13.7° (± 15.7) in the axial, sagittal, and coronal planes.	Prospective Level II
Brussens et al.,[33]	P (n = 30)	Quantified the reliability of a novel measurement method by hindfoot alignment angle and talar shift.	Improved spatial interpretability and definition of alignment.	Relationship between novel angle and the talar shift = 0.87; Novel hindfoot alignment angle coefficient = 0.72.	Retrospective Level III
Burssens et al.,[34]	P (n = 18)	Assessed the hind- and midfoot alignment after medializing calcaneal osteotomy.	Improved spatial interpretability and definition of alignment.	Hindfoot angle improved preoperative. In addition, navicular height, rotation, and Meary's angle improved.	Prospective Level II
Lintz et al.,[35]	P(n = 189)	Analyzed hindfoot alignment by FAO in patients.	Improved definition of alignment.	Mean FAO was −2.2% ± 5.5% (varus) and + 2.6% ± 4.7% (valgus) with and without lateral ankle instability history.	Retrospective Level III
Lintz et al.,[36]	P (n = 78) HI (n = 57)	Measured the FAO for patients with hindfoot disorders.	Improved spatial interpretability and definition of alignment.	In standard cases, the mean value for FAO was 2.3% ± 2.9%, whereas, in varus and valgus cases, the mean was −11.6% ± 6.9% and 11.4% ± 5.7%.	Retrospective Level III
de Cesar Netto et al.,[37]	P (n = 45)	Hindfoot alignment in National Basketball Association players with different symptomatic foot and ankle injuries.	Improved spatial interpretability and definition of alignment.	The mean FAO was 0.48; the mean hindfoot alignment angle was 1.42° (−0.80–3.65°). The mean Inftal-Suptal grade was 5.31° (3.50°–7.12°), while the mean Inftal-Hor grade was 4.04° (2.56°–5.51°).	Retrospective Level III
Bernasconi et al.,[38]	P (n = 34) H (n = 17)	Assessed the reliability of semi-automatic measurements in symptomatic pes cavovarus.	Improved spatial interpretability and definition of alignment.	Mean values for intra and interobserver reliability for FAO (r = 0.98; ICC: 0.99), calcaneal offset (r = 0.97; ICC: 0.98) and hindfoot alignment angle measurements (r = 0.97; ICC: 0.98) were excellent.	Retrospective Level III
Burssens et al.,[39]	P (n = 48)	Assessed the hindfoot alignment using WBCT for the foot with valgus.	Improved definition of alignment.	The mean hindfoot alignment equalled 0.79° of valgus ± 3.2 with a mean tibia axis of 2.7° varus ± 2.1.	Retrospective Level III
Patel et al.,[40]	P (n = 33)	Analysed the reliability of foot posture index in define foot alignment.	Improved spatial interpretability and definition of alignment.	The foot posture index demonstrated excellent intra-rater and good inter-rater reliability.	Retrospective Level III
Day et al.,[41]	P (n = 21)	Quantified 3D measures of subtalar joint space width with intra-articular calcaneal fractures.	Improved spatial interpretability, area and volume measurements, and novel 3D measurements.	Mean 3D joint space width values for patients ranged from 0.9 to 2.5 mm (1.7 ± 0.4 mm) over the entire subtalar joint. In addition, mean and minimum 3D joint space width values correlated inversely with visual analogue scale pain scores and Kellgren-Lawrence grade.	Prospective Level III
Progressive Collapsing Foot Deformity (PCFD)					
Fuller et al.,[42]	P (n = 71)	Tested the reliability of WBCT in 6 radiographic parameters of PCFD.	Improved definition of alignment.	Measurements demonstrated excellent interrater reliability and were suitable for an excellent interrater agreement.	Retrospective Level III
Auch et al.,[43]	P (n = 62) HI (n = 29)	Measured FAO and distal tibiofibular syndesmosis area in PCFD.	Improved evaluation of joint space width.	DTFS area measurements increased a mean of approximately 10 mm^2 compared to controls. A significantly weak positive	Retrospective Level III

(*continued on next page*)

Table 2 (*continued*)

Study	Subjects	Diagnostic applications	Potential benefits	Findings	Level of evidence
				correlation was found between FAO and DTFS area measurements, with the highest syndesmotic widening occurring when FAO values were between 7% and 9.3%.	
Lintz et al.,[44]	P (n = 28) HI (n = 28)	Measured middle facet incongruence angle (MF°) and uncoverage percentage (MF%) and FAO for diagnosing PCFD.	Improved spatial interpretability and evaluation of joint space width.	MF% and FAO were both accurate measurements for PCFD. MF% demonstrated slightly better specificity. FAO better sensitivity.	Retrospective Level III
de Cesar Netto et al.,[45]	P (n = 30) HI (n = 30)	Measured the amount of subluxation (percentage of uncoverage) and the incongruence angle of the middle facet in PCDF.	Improved evaluation of joint space width.	The middle facet demonstrated significantly increased progressive peritalar subluxation in patients with PCFD. With a mean value for joint uncoverage of 45.3% compared with 4.8% in controls. A significant difference was also found for the incongruence angle, with a mean value of 17.3° in the PCFD group and 0.3° in controls.	Retrospective Level III
Lalevée et al.,[46]	P (n = 72)	Assessed the prevalence of sinus tarsi, talus-fibular and calcaneo-fibular in PCFD and their association with peritalar subluxation.	Improved evaluation of joint space width.	Sinus tarsi and talus-fibular were more prevalent than calcaneo-fibular in PCFD. However, only sinus tarsi was associated with peritalar subluxation.	Retrospective Level III
de Cesar Netto et al.,[47]	P (n = 54)	Evaluated the relationship between bone alignment and soft tissue injury in PCFD.	Improved evaluation of joint space width.	The posterior tibial tendon was associated with sinus tarsi impingement; Spring ligaments were associated with subtalar subluxation; The calcaneal ligament was associated with subfibular impingement.	Retrospective Level III
Krähenbühl et al.,[48]	P (n = 20) H (n = 30)	Assessed medial facet subluxation and sinus tarsi/ subfibular impingement in PCDF.	Improved spatial interpretability and definition of alignment.	The medial facet subluxation correlates with 3D measures; Sinus tarsi impingement correlates with soft tissue degeneration.	Retrospective Level III
Kim et al.,[49]	P (n = 91)	Measured the distance between talocalcaneal and calcaneofibular to detect bony impingement in PCDF.	Improved definition of alignment.	Talocalcaneal distance narrowing at the sinus tarsi strongly correlated with talonavicular coverage angle; A talonavicular coverage angle threshold of 41.2° had a 100% positive predictive value for predicting sinus tarsi impingement, hindfoot moment arm threshold of 38.1 mm had a 100% positive predictive value for calcaneofibular impingement.	Retrospective Level III
Jeng et al.,[50]	P (n = 25)	Assessment of bony subfibular impingement in PCDF.	Improved evaluation of joint space width.	35% of flatfoot patients with posterior tibial tendonitis had bony impingement between the fibula and calcaneus on the coronal view. 38% had bony impingement between the talus and calcaneus on the sagittal view.	Retrospective Level III
de Cesar Netto et al.,[51]	P (n = 76)	Assessment of posterior and middle facet subluxation of the subtalar joint in PCDF.	Improved spatial interpretability and evaluation ofjoint space width.	Measurements of middle facet subluxation were significantly higher than those for posterior facet subluxation; For every 1% increase in posterior facet subluxation, there was a corresponding 1.6-fold increase in middle facet subluxation.	Retrospective Level III
de Cesar Netto et al.,[52]	P (n = 20)	Compared clinical and WBCT assessment of hindfoot alignment in PCFD.	Improved spatial interpretability and definition of alignment.	It was significantly different clinical and WBCT assessment: The mean of clinically measured hindfoot valgus was 15.2°; WBCT measurements: Clinical hindfoot alignment Angle, 9.9°.	Prospective Level II
Shakoor et al.,[53]	P (n = 20)	Compared and validated PCFD measurements between WBRX and WBCT images.	Improved spatial interpretability and definition of alignment.	Except for medial-cuneiform-first-metatarsal-angle, adequate intra-observer reliability (range:0.61–0.96) was observed for weightbearing radiographic measurements. Moderate to very good interobserver reliability between weightbearing radiograph and weightbearing CBCT measurements.	Prospective Level III
de Cesar Nettoe t al.,[54]	P (n = 113)	Evaluated the reliability of semiautomatic measurements in measure FAO and foot arch angle in PCDF.	Improved spatial interpretability and definition of alignment.	FAO semiautomatic measurements demonstrated excellent intra- and interobserver reliabilities; Foot arch angle were the only variables found to significantly influence and correlate with FAO measurements.	Retrospective Level III
Day et al.,[55]	P (n = 19)	Measured FAO pre-and post-operative in PCDF.	Improved spatial interpretability and definition of alignment.	Mean preoperative FAO of 9.8% to a mean postoperative value of 1.3%.	Prospective Level II
Behrens et al.,[56]	P (n = 20) HI (n = 20)	Evaluated the talonavicular and calcaneocuboid interfaces by distance and coverage mapping techniques in PCDF.	Improved spatial interpretability, evaluation of joint space width, and novel 3D measurements.	Talar head coverage decreases in plantarmedial and dorsalmedial regions were seen with corresponding increases in plantarlateral and dorsolateral regions in PCFD. Calcaneocuboid coverage decreased in plantar and medial regions and increased in the lateral region.	Retrospective Level III
Dibbern et al.,[57]	P (n = 20) H (n = 10)	Assessed peritalar subluxation in patients with PCFD using 3D distance mapping.	Improved spatial interpretability and novel 3D measurements.	Coverage was decreased in articular regions and impingement was increased in nonarticular regions of patients with PCFD with a	Retrospective Level III

(*continued on next page*)

Table 2 (*continued*)

Study	Subjects	Diagnostic applications	Potential benefits	Findings	Level of evidence
				significant increase in uncoverage in the middle (46.6%) but not anterior or posterior facets.	
de Cesar Netto et al.,[58]	P (n = 20)	Assessed PCFD in the sagittal, coronal, and axial planes using CT while weightbearing and non-weightbearing.	Improved spatial interpretability and definition of alignment.	The difference between weightbearing and non-weightbearing images, were the medial cuneiform-to-floor distance and the forefoot arch angle in the coronal view and the cuboid-to-floor distance and the navicular-to-floor distance in the sagittal view.	Retrospective Level II.
Charcot-Marie-Tooth					
Michalski et al.,[62]	P (n = 20) HI (n = 20)	Quantified morphologic differences of the calcaneus and talus in Charcot-Marie-Tooth disease.	Improved spatial interpretability and definition of alignment.	Charcot-Marie-Tooth disease patients had significantly less talar sagittal declination vs controls (17.8° vs 25.1°); The calcaneal radius of curvature in patients was considerably smaller than in controls (822.8 vs 2143.5 mm).	Retrospective Level III
An et al.,[63]	P (n = 21) HI (n = 20)	Quantified the axial and rotational alignment in Charcot-Marie-Tooth disease.	Improved spatial interpretability and Improved quantification of rotation.	Maximal rotational deformity in Charcot-Marie-Tooth disease patients occurred at the transverse tarsal joints, averaging 61° of external rotation (supination), compared to 34° among controls.	Retrospective Level III
Sangoi et al.,[64]	P (n = 16) HI (n = 16)	Assessed differences in measurements done manually on 2D slices of WBCT vs 3D computer models in normal and Charcot-Marie-Tooth disease.	Improved spatial interpretability definition of alignment.	Automated assessment calculated increased sagittal plane deformity (fixed bias 7.31° for Meary's angle, 2.39° for calcaneal pitch) and less axial plane deformity (fixed bias 10.61° for axial talar–first metatarsal angle) than controls.	Retrospective Level III

Abbreviations: P, patients; HI, healthy Individuals; 2D, two-dimensional; 3D, three-dimensional; ICC, intra class correlation coefficient; FAO, foot and ankle offset; PCFD, progressive collapsing foot deformity; MF%, middle facet incongruence angle; WBCT, weightbearing CT.

Table 3
Literature review of midfoot studies.

Study	Subjects	diagnostic applications	Potential benefits	Findings	Level of evidence
Lisfranc injury					
Sripanich et al.,[65]	P (n = 96)	Measured the distance between the medial cuneiform and second metatarsal to assess the Lisfranc joint using WBCT imaging.	Improved evaluation of joint space width.	Measuring the medial cuneiform and second metatarsal joint space with coronal WBCT imaging through a protocol that localizes the interosseous Lisfranc ligament is reproducible.	Retrospective Level III
Falcon et al.,[66]	P (n = 56)	Measured the Lisfranc joint between injured and uninjured side.	Improved evaluation of joint space width.	Patients with Lisfranc complex had a larger M1-M2 base distance and M2-C1 interval compared to uninjured side. Males had significantly higher M2-C1, intercuneiform distance, and sagittal descent compared to female patients.	Retrospective Level III
Bhimani et al.,[67]	P (n = 16) HI (n = 36)	Analyzed the diagnostic sensitivities of 3D volumetric measurement of the injured Lisfranc joint complex.	Improved spatial interpretability and area and volume measurements.	Volumetric measurement sensitivity (coronal (92.3%) and axial (91.6%) plane) and specificity (coronal (97.7%) and axial (96.5%) plane).	Diagnostic Level III
Midfoot Osteoarthritis					
Steadman et al.,[68]	P (n = 302)	Assessed diagnostic sensitivity of midfoot osteoarthritis by 3 midfoot joint groups (Chopart, "central", and tarsometatarsal).	Improved evaluation of joint space width.	Diagnostic sensitivity (72.5%) and specificity (87.9%) for Chopart joints; Sensitivity (61.5%), specificity (96.1%) for central joints; Sensitivity (68.4%), and specificity (92.9%) for tarsometatarsal joints.	Retrospective Level III

Abbreviations: P, Patients; HI, healthy individuals; 3D, three-dimensional; M1, first metatarsal; M2, second metatarsal; WBCT, weightbearing CT;
C1, medial cuneiform.

Table 4
Literature review of forefoot studies.

Study	Subjects	Diagnostic applications	Potential benefits	Findings	Level of evidence
Hallux Valgus					
Mansur et al.,[69]	P (n = 26) HI (n = 20)	Measured rotation of M1 in WBRX and WBCT.	Improved quantification of rotation.	Hallux valgus angle was higher in WBCT than WBRX in metatarsal rotation angle, head diameter, and sesamoid rotation angle.	Retrospective Level III
Zhong Et al.,[70]	P (n = 26)	Analyzed distal metatarsal articular angle in WBRX and WBCT.	Improved spatial interpretability and definition of alignment.	A mean difference of 0.11 ± 2.42° between WBCT and WBRX.	Retrospective Level III
Lalevée et al.,[71]	P (n = 27) HI (n = 16)	Compared the distal metatarsal articular angle in HV and control populations	Improved spatial interpretability and definition of alignment.	Although the valgus deformity of M1 distal articular surface in hallux valgus is overestimated on conventional radiographs, comparing to controls showed that an 8.6° increase remained after confounding factors' correction.	Retrospective Level III
Najefi et al.,[72]	P (n = 102)	Analyzed the relationship between intermetatarsal angle, metatarsal pronation angle, and hindfoot alignment angle.	Improved quantification of rotation.	Strong positive correlation between sesamoid rotation angle and hallux valgus angle/intermetatarsal angle; Weakly correlated between metatarsal pronation angle/alpha angle and hallux valgus angle/ intermetatarsal angle.	Retrospective Level IV
Clarke et al.,[73]	P (n = 38) HI (n = 10)	Measured crista volume, sesamoid station, and M1 pronation in hallux valgus.	Improved spatial interpretability and area and volume measurements.	The mean crista volume in hallux valgus patients was 80.10 ± 35 mm^3; Decreasing crista volumes significantly and strongly correlated with increasing sesamoid station.	Retrospective Level III
Mahmoud et al.,[74]	P (n = 20)	Analyzed the M1 pronation angle.	Improved quantification of rotation.	Alpha angle has a relationship with tibial sesamoid subluxation and only trended toward a weak linear relationship with intermetatarsal angle.	Retrospective Level III
Lee et al.,[75]	P (n = 25)	Assessed metatarsus primus elevatus in the hallux rigidus.	Improved definition of alignment.	The metatarsus primus elevatus threshold for hallux rigidus diagnosis was 4.19 mm with 77% sensitivity and 77% specificity.	Prospective Level III
Carvalho et al.,[76]	P (n = 19)	Assessed the reliability of WBCT computer-assisted semi-automatic imaging measurements in hallux valgus.	Improved spatial interpretability.	Reliabilities utilizing ICC were over 0.80 for WBCT manual measurements and WBCT semi-automatic measurements.	Retrospective Level III
Lee et al.,[75]	P (n = 53) HI (n = 30)	Analyzed signs of instability of the first tarsometatarsal joint.	Improved definition of alignment.	The hallux valgus group demonstrated instability mainly in sagittal and axial planes; the hallux rigidus group had sagittal instability predominantly.	Retrospective Level III
Day et al.,[77]	P (n = 68) HI (n = 58)	Evaluated automatic measurement for the M1-M2 intermetatarsal angle in hallux valgus.	Improved spatial interpretability.	Measurements generated by the WBCT artificial intelligence-based automatic measurement system for intermetatarsal angle demonstrated strong correlations with manual measures, with near-perfect reproducibility.	Retrospective Level III
Conti et al.,[78]	P (n = 30)	Measured the pronation of the M1 after the modified Lapidus procedure.	Improved spatial interpretability and quantification of rotation.	The average decrease in the M2 from preoperatively to postoperatively was 5.9°; The α angle also significantly decreased from preoperatively to postoperatively (10.5°).	Retrospective Level III
Conti et al., [79]	P (n = 30)	Analysed the foot width in patients after the modified Lapidus.	Improved evaluation of joint space width.	Bony foot width decreased significantly by a mean of 8.9 mm (9.1%) on WBRX and 7.9 mm (8.4%) on WBCT scans.	Retrospective Level III
Conti et al.,[80]	P (n = 31)	Investigated pronation of the M1 after the modified Lapidus.	Improved spatial interpretability and quantification of rotation.	The mean pre- and postoperative pronation of the hallux valgus angle was 29.0° and 20.2°; The average pre- and postoperative intermetatarsal angle was 16.7° and 8.8°.	

Abbreviations: P, patients; HI, healthy individuals; ICC, intra class correlation coefficient; M1, first metatarsal; M2, second metatarsal; WBCT, weightbearing CT; WBRX, weightbearing radiographs.

and tarsometatarsal arthritis and reported that WBCT imaging facilitates an earlier, more reliable diagnosis and grading of midfoot osteoarthritis relative to WBRX.

3.4. Forefoot

A total of nineteen studies [69–87] reported on forefoot disorders (Table 4), these studies used 2D or 3D variables to diagnose and quantify hallux valgus deformity. In studies [69,72,74–76,79] using 2D measurement variables, WBCT mainly focused on quantifying first metatarsal (M1) alignment [75,76,79] and rotation [69,72,74]. Mansur et al. [69] evaluated the accuracy of various radiographic measurements in diagnosing hallux valgus deformity; Najefi et al. [72], using WBCT-assessed hallux valgus and metatarsal rotation angles; Mahmoud et al. [74] measured several angles, including the first-second intermetatarsal angle, hallux valgus angle, Meary's angle, and calcaneal pitch angle. Their study reported that WBCT can be a valuable tool for quantifying M1 pronation. Conti et al. [79] investigated changes in foot width following pre- compared to post-operatively for the patients with hallux valgus and reported that the modified Lapidus can effectively decrease foot width.

In studies [70,71,73,76–78,80–82] using 3D measurement variables, Zhong et al. [70] reconstructed 3D models to improve spatial interpretability, when measuring hallux valgus and the distal metatarsal articular angle. Lalevée et al. [71] utilized WBCT to correct the pronation and plantarflexion of the M1 and compared the 3D distal metatarsal articular angle in patients with hallux valgus deformity and control populations. They [71] reported that conventional radiographs overestimate the valgus deformity of the M1 distal articular surface. Finally, Carvalho et al. [76] measured the hallux valgus angle and Day et al. [77] used WBCT to measure the forefoot on artificial intelligence–based measurement. Their [76,77] studies reported that 3D measurements are more reliable and accurate than 2D measurements.

3.5. Imaging and segmentation time, radiation dose and costs

A total of 2 studies were identified that investigated radiation dose, time spent on image acquisition, and cost-effectiveness [84,85]. Richter et al. [84] reported that the time spent for the WBCT was 70% faster than radiographs and 35% faster than CT scan, because no changes in patient positioning was required. In a second study, Richter et al. [85], analyzed 11,009 WBCT scans over 5.6 years to assess the potential benefit of using WBCT over WBRX and/or CT as the standard imaging modality. They reported there was a 10% decreased in radiation dose, 77% decrease in image acquisition time and increased financial profit for the institution.

A total of 2 studies [86,87] compared the time to segment CT data using automated versus manual measurements and obtain accurate results in 5 angles of the foot and ankle. Investigators reportedly spent 73% less time than manual measurements (44.5 s per angle) using the semi-automated measurement software (12 s per angle) (Bonelogic Ortho Foot and Ankle, Version 1.0.0-R, Disior Ltd, Helsinki, Finland) [86]; Full-Automated measurement (automatically generate 3D models and identify different bones) software (1 s per angle) (AM, Autometrics, Curvebeam, Warrington, PA, USA) reduced measurement time by 97% compared to manual measurements (44.5 s per angle) [87].

4. Discussion

The principal finding of this systematic review identified a growing diagnostic landscape for applications of WBCT, which was most frequently studied in hindfoot deformities (Table 2). Compared to WBRX, the most commonly reported diagnostic applications of WBCT imaging were improved spatial interpretability to quantify structural and rotational deformities, amongst others due to 3D reconstruction (Table 5, Figs. 2–4), and the benefits were time spent on image acquisition, radiation dose, and the cost-effectiveness of using WBCT compared to WBRX or traditional CT [84,85]. Off note, one additional value of 3D reconstructions is to allow (semi-)automated measurements. These have shown to reduce the measurement time, but reported also different values compared to manual measurements [86,87]. This should be taken in to account when performing (semi-)automated measurements and needs further investigation in future studies.

Specifically, in the ankle, WBCT showed higher accuracy for quantifying alignment, ankle joint space width for patients with osteoarthritis [11,14,16] or tibiofibular distance in syndesmotic ankle injuries [19,20,22] using both 2D and 3D measurements. Although the consensus in these studies points towards the benefits of WBCT in ankle disorders, it should be taken into account that the level of evidence was moderate. The mean MINORS of the 14 studies in the ankle was equalled 10.1 on a total of 24, and twelve studies are level III of the evidence, and two studies are level IV.

In the hindfoot, WBCT is a valuable tool for accurately quantifying the hindfoot alignment [25,28,29,36,38,41]. Measurements were not significantly affected by the presence of hardware [29,33,37], anatomic variability [28,30], and projection or orientation [31,34–36,41] when compared to WBRX. In particular, the reconstructed 3D models of the talus and calcaneus allowed also to quantify 3D talocalcaneal alignment of the subtalar joint [25,28,34,56,57,62,63]. To overcome the inability of WBCT to assess soft tissue structures, one study combined WBCT and MRI to evaluate hindfoot disorders, with a good correlation between both modalities [47]. The level of evidence was in the same range as the ankle studies and demonstrate mean MINORS of the 41 studies in the hindfoot was equalled 9.7 on a total of 24, thirty-four studies are level III of the evidence, and seven studies are level II.

In the midfoot, WBCT overcame the superposition of the bones and improved the characterization of the 3D structural details [67,68]. Assessing the Lisfranc joint complex under physiological load allowed to effectively differentiate between stable and unstable Lisfranc injuries [65,67] and determine joint space changes for patients with ligamentous disruption, especially in subtle cases [66]. Additionally, midfoot osteoarthritis is often missed or underestimated on WBRX [68]. WBCT allowed for an earlier and more reliable diagnosis of midfoot osteoarthritis than WBRX [68]. The mean MINORS of the 4 studies in the midfoot was equalled 9.5 on a total of 24; Four studies were level III of the evidence. Of note, the mean MINORS was the lowest among the studies assessing the midfoot, indicating that this anatomical area would benefit more from higher-quality studies.

In the forefoot, WBCT allowed the assessment of the bone in coronal, axial, and sagittal planes to determine rotation, varus/valgus, and plantarflexion [70,71,74,77]. The ability to accurately and reliably quantify M1 pronation is an important step to help surgeons acquire more optimal corrections and maximize functional results [69,72]. Unfortunately, an accurate linear evolution of hallux valgus could not be evaluated due to the retrospective nature of the studies [75]. In addition, there is no "gold standard" [78] for the measurement of M1 rotation and sesamoid pronation [74,75]. The mean MINORS of the 17 studies in the forefoot was equalled 10.2 on a total of 24, sixteen studies are level III of the evidence, and one studies are level IV.

Table 5
List of potential benefits.

Benefits	Number of studies		Reference of studies
Absence of superposition			
Improved evaluation of joint space width	18	Ankle	10,15,17,21–23
		hindfoot	43–47,50,51,56
		Midfoot	65,66,68
		Forefoot	79
Improved quantification of rotation	8	Ankle	11,13,20
		hindfoot	
		midfoot	62
		forefoot	68,71,74,80
Improved definition of alignment	36	ankle	12,14,16,18
		hindfoot	25–28,30–40,42,49,52–55,58,59,62,63,64,70,71,75
		midfoot	
		forefoot	76,79
Availability of 3D reconstructions			
Area and volume measurements	5	ankle	20,21
		hindfoot	41
		midfoot	66
		forefoot	72
Improved spatial interpretability	36	ankle	18,20,21,
		hindfoot	24,25,28–30,32–34,36–38,40,41,44,48,51–64
		midfoot	67
		forefoot	70,71,73,76–78,80,81;82
Novel 3D measurements (3D distance map)	5	ankle	19
		hindfoot	34,41,47,56,57,60–62
		midfoot	
		forefoot	
Reduced imaging time	4		83,84,85,86
Reduced costs	2		83,84
Radiation dose	1		84

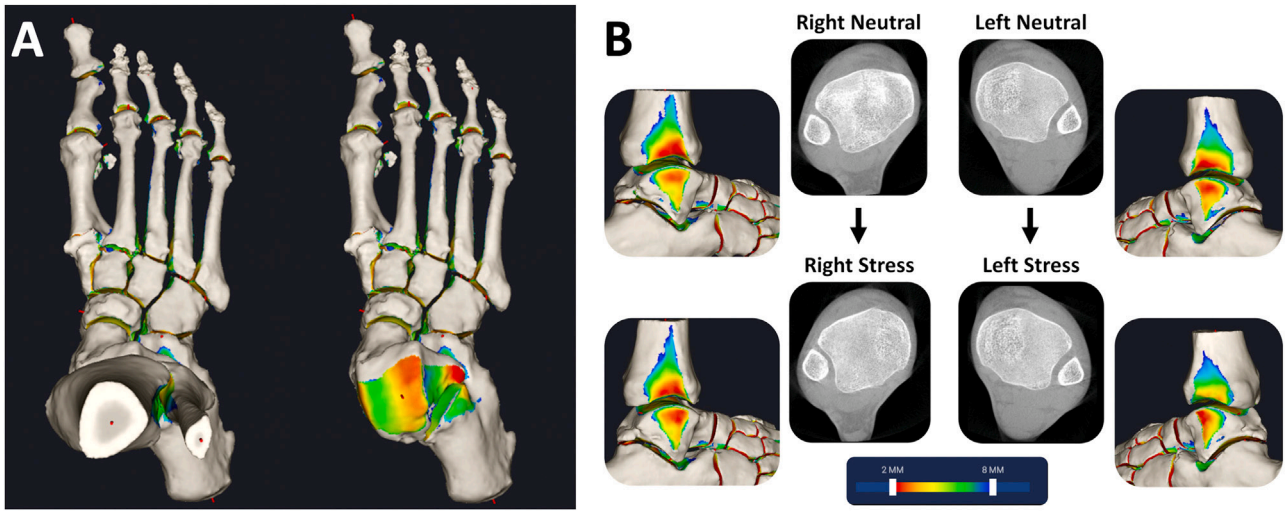

Fig. 4. Examples of distance mag analysis using Disior® software (Paragon 28, Denver, US) (A) Patient with ankle valgus deformity demonstrating a lateral overload in the ankle joint (B) weightbearing CT (WBCT) images in neutral stance (upper) and augmented external rotation stress (lower) in a patient with a syndesmotic injury in the left ankle. For each condition, a corresponding 3D distance mapping plot is presented, which reveals an increased tibiofibular clear space on the left side during external rotation stress as described by Peiffer et al. [94].

This study contained several important limitations. Firstly, some publications may not have been identified with the applied search strategy. This could be attributed to the chosen search terms or the fact that studies that were not written in English were excluded. To minimize error, all references of included studies were additionally screened. Secondly, the results and conclusions were based on a limited number of studies with heterogeneous study designs. Furthermore, since there were considerable differences in the reported radiological and clinical outcomes, we were unable to perform a meta-analysis assessing the general effect of WBCT on the alignment of the ankle and foot. Thirdly, 22 out of the 76 studies presented a relatively low study quality, which could impede the generalizability of the obtained findings.

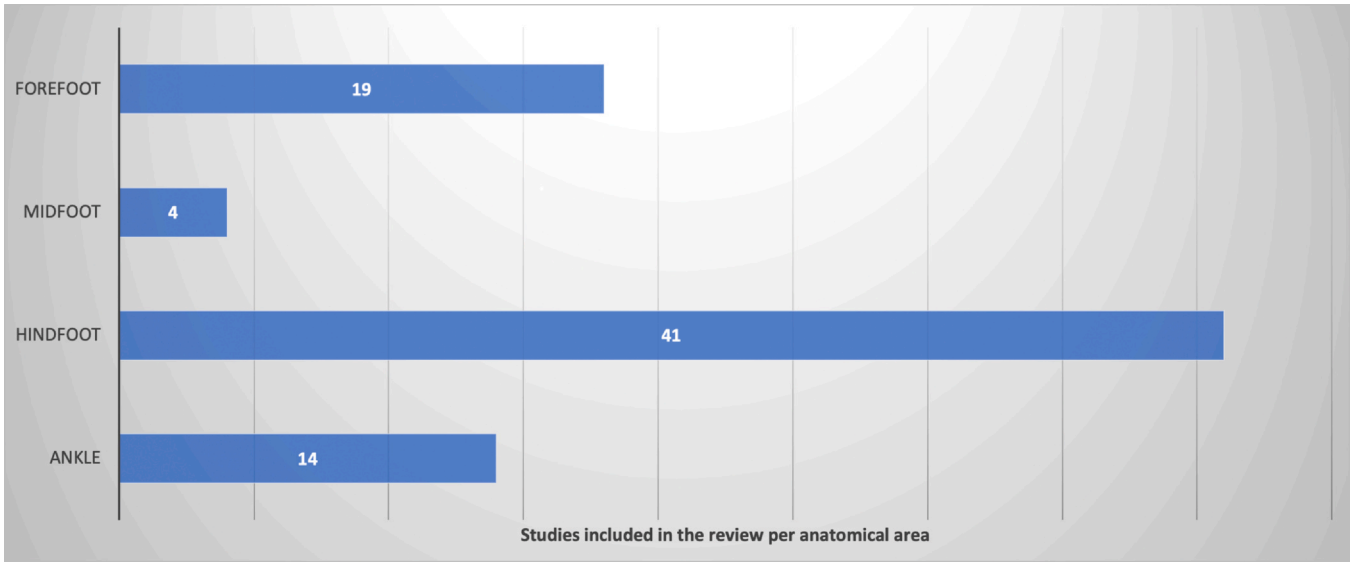

Fig. 5. Number of weightbearing CT (WBCT) studies per anatomical area the in foot and ankle.

5. Conclusion

Diagnostic applications of WBCT imaging are, at present, most frequently studied in hindfoot deformity, but other areas are on the rise due to rapid growth in the number of indications (Fig. 5). Definition of alignment, evaluation of joint width and spatial interpretability of images in 3D were identified as the main benefits compared to WBRX. This study was to first review the WBCT literature according to a systematic approach over the last ten years. The identified applications of WBCT can help orthopaedic surgeons to evaluate various disorders of the foot and ankle by avoiding measurement errors caused by patient positioning and osseous superimposition. Hereby, weightbearing CT is able to surmount the diagnostic information obtained from weightbearing X-ray's [8,84]. With the continuous application of WBCT, corresponding software will be developed to facilitate measurement methods in both 2D and 3D [91]. Moreover, weight-bearing CT could further progress as standard imaging tool in the diagnostic work-up of foot and ankle disorders, since it is also capable of providing digitally reconstructed radiographs (DDRs) from the CT images [92,93]. However, the obtained findings should be interpreted with caution as the average quality score was moderate. Therefore, future prospective studies with adequate sample sizes are warranted to standardize the measurement terminology and consolidate the role of WBCT in diagnostic and therapeutic algorithms.

References

[1] Shereff MJ, DiGiovanni L, Bejjani FJ, Hersh A, Kummer FJ. A comparison of non-weightbearing and weight-bearing radiographs of the foot. Foot Ankle Int 1990;10(6):306–11. https://doi.org/10.1177/107110079001000604
[2] Kumar V, Baburaj V, Patel S, Sharma S, Vaishya R. Does the use of intraoperative CT scan improve outcomes in Orthopaedic surgery? A systematic review and meta-analysis of 871 cases. J Clin Orthop Trauma 2021;18:216–23. https://doi.org/10.1016/j.jcot.2021.04.030
[3] Brian CL, Allahabadi S, Palanca A, Oji DE. Understanding radiographic measurements used in foot and ankle surgery. J Am Acad Orthop Surg 2022;30(2):e139–54. https://doi.org/10.5435/JAAOS-D-20-00189
[4] Cifuentes-De la Portilla C, Larrainzar-Garijo R, Bayod J. Analysis of the main passive soft tissues associated with adult acquired flatfoot deformity development: a computational modeling approach. J Biomech 2019;84:183–90. https://doi.org/10.1016/j.jbiomech.2018.12.047
[5] Godoy-Santos AL, Netto C, de C. Weight-bearing computed tomography of the foot and ankle: an update and future directions. Acta Ortop Bras 2018;26(2):135–9. https://doi.org/10.1590/1413-785220182602188482
[6] De Bruijn J, Hagemeijer NC, Rikken QGH, Husseini JS, Saengsin J, Kerkhoffs GMMJ, Waryasz G, Guss D, DiGiovanni CW. Lisfranc injury: Refined diagnostic methodology using weightbearing and non-weightbearing radiographs. 2022 Injury 2022;53(6):2318–25. https://doi.org/10.1016/j.injury.2022.02.040
[7] Godoy-Santos AL, Bernasconi A, Bordalo-Rodrigues M, Lintz F, Teixeira Lôbo CF, De Cesar Netto C. Weight-bearing cone-beam computed tomography in the foot and ankle specialty: where we are and where we are going – an update. Radio Bras 2021;54(3):177–84. https://doi.org/10.1590/0100-3984.2020.0048
[8] Lintz F, Netto C, de C, Barg A, Burssens A, Richter M. Weight-bearing cone beam CT scans in the foot and ankle. EFORT Open Rev 2018;3(5):278–86. https://doi.org/10.1302/2058-5241.3.170066
[9] Brinch S, Wellenberg RHH, Boesen MP, et al. Weight-bearing cone-beam CT: the need for standardised acquisition protocols and measurements to fulfill high expectations—a review of the literature. Skelet Radio 2023;52(6):1073–88. https://doi.org/10.1007/s00256-022-04223-1
[10] Willey MC, Compton JT, Marsh JL, et al. Weight-bearing CT scan after tibial pilon fracture demonstrates significant early joint-space narrowing. J Bone Jt Surg - Am Vol 2020;102(9):796–803. https://doi.org/10.2106/JBJS.19.00816
[11] Hintermann B, Susdorf R, Krähenbühl N, Ruiz R. Axial rotational alignment in mobile-bearing total ankle arthroplasty. Foot Ankle Int 2020;41(5):521–8. https://doi.org/10.1177/1071100720902838
[12] Krähenbühl N, Tschuck M, Bolliger L, Hintermann B, Knupp M. Orientation of the subtalar joint: Measurement and reliability using weightbearing CT scans. Foot Ankle Int 2016;37(1):109–14. https://doi.org/10.1177/1071100715600823
[13] Kim JB, Yi Y, Kim JY, et al. Weight-bearing computed tomography findings in varus ankle osteoarthritis: abnormal internal rotation of the talus in the axial plane. Skelet Radio 2017;46(8):1071–80. https://doi.org/10.1007/s00256-017-2655-0
[14] Kang HW, Kim DY, Park GY, Lee DO, Lee DY. Coronal plane calcaneal-talar orientation in varus ankle osteoarthritis. Foot Ankle Int 2022;43(7):928–36. https://doi.org/10.1177/10711007221088566
[15] Kim JB, Chul, Park H, Ahn JY, Kim J, Lee WC. Characteristics of medial gutter arthritis on weightbearing CT and plain radiograph. Skelet Radio 2022;43(7):928–36. https://doi.org/10.1007/s00256-020-03688-2
[16] Krähenbühl N, Siegler L, Deforth M, Zwicky L, Hintermann B, Knupp M. Subtalar joint alignment in ankle osteoarthritis. Foot Ankle Surg 2019;25(2):143–9. https://doi.org/10.1016/j.fas.2017.10.004
[17] Patel S, Malhotra K, Cullen NP, Singh D, Goldberg AJ, Welck MJ. Defining reference values for the normal tibiofibular syndesmosis in adults using weight-bearing CT. Bone Jt J 2019;3:348–52. https://doi.org/10.1302/0301-620X.101B2
[18] Peiffer M, Burssens A, De Mits S, et al. Statistical shape model-based tibiofibular assessment of syndesmotic ankle lesions using weight-bearing CT. J Orthop Res 2022;40(12):2873–84. https://doi.org/10.1002/jor.25318
[19] Malhotra K, Welck M, Cullen N, Singh D, Goldberg AJ. The effects of weight bearing on the distal tibiofibular syndesmosis: a study comparing weight bearing-CT with conventional CT. Foot Ankle Surg 2019;25(4):511–6. https://doi.org/10.1016/j.fas.2018.03.006
[20] Ashkani Esfahani S, Bhimani R, Lubberts B, et al. Volume measurements on weightbearing computed tomography can detect subtle syndesmotic instability. J Orthop Res 2022;40(2):460–7. https://doi.org/10.1002/jor.25049
[21] Shakoor D, Osgood GM, Brehler M, et al. Cone-beam CT measurements of distal tibiofibular syndesmosis in asymptomatic uninjured ankles: does weight-bearing matter? Skelet Radio 2019;48(4):583–94. https://doi.org/10.1007/s00256-018-3074-6
[22] del Rio A, Bewsher SM, Roshan-Zamir S, et al. Weightbearing cone-beam computed tomography of acute ankle syndesmosis injuries. J Foot Ankle Surg 2020;59(2):258–63. https://doi.org/10.1053/j.jfas.2019.02.005

[23] Rooney P, Haller J, Kleweno C, et al. Syndesmosis malposition assessed on weight-bearing CT is common after operative fixation of intra-articular distal tibia plafond fracture. J Orthop Trauma 2022;36(12):658–64. https://doi.org/10.1097/BOT.0000000000002443

[24] Zhang JZ, Lintz F, Bernasconi A, Zhang S. 3D biometrics for hindfoot alignment using weightbearing computed tomography. Foot Ankle Int 2019;40(6):720–6. https://doi.org/10.1177/1071100719835492

[25] Burssens A, Susdorf R, Krähenbühl N, et al. Supramalleolar osteotomy for ankle varus deformity alters subtalar joint alignment. Foot Ankle Int 2022;43(9):1194–203. https://doi.org/10.1177/10711007221108097

[26] Bernasconi A, Netto CDC, Roberts L, Lintz F, Godoy-Santos AL, O'Malley MJ. Foot alignment in symptomatic national football league (NFL) athletes: a weight-bearing Ct analysis. Acta Ortop Bras 2021;29(3):118–23. https://doi.org/10.1590/1413-785220212903236709

[27] Hirschmann A, Pfirrmann CWA, Klammer G, Espinosa N, Buck FM. Upright cone CT of the hindfoot: comparison of the non-weight-bearing with the upright weight-bearing position. Eur Radio 2014;24(3):553–8. https://doi.org/10.1007/s00330-013-3028-2

[28] Burssens A, Peeters J, Peiffer M, et al. Reliability and correlation analysis of computed methods to convert conventional 2D radiological hindfoot measurements to a 3D setting using weightbearing CT. Int J Comput Assist Radio Surg 2018;13(12):1999–2008. https://doi.org/10.1007/s11548-018-1727-5

[29] Lintz F, Ricard C, Mehdi N, et al. Hindfoot alignment assessment by the foot–ankle offset: a diagnostic study. Arch Orthop Trauma Surg Publ Online 2022;143(5):2373–82. https://doi.org/10.1007/s00402-022-04440-2

[30] Arena CB, Sripanich Y, Leake R, Saltzman CL, Barg A. Assessment of hindfoot alignment comparing weightbearing radiography to weightbearing computed tomography. Foot Ankle Int 2021;42(11):1482–90. https://doi.org/10.1177/10711007211014171

[31] Bakshi N, Steadman J, Philippi M, et al. Association between hindfoot alignment and first metatarsal rotation. Foot Ankle Int 2022;43(1):105–12. https://doi.org/10.1177/10711007211033514

[32] Peiffer M, Belvedere C, Clockaerts S, et al. Three-dimensional displacement after a medializing calcaneal osteotomy in relation to the osteotomy angle and hindfoot alignment. Foot Ankle Surg 2020;26(1):78–84. https://doi.org/10.1016/j.fas.2018.11.015

[33] Burssens A, Peeters J, Buedts K, Victor J, Vandeputte G. Measuring hindfoot alignment in weight bearing CT: a novel clinical relevant measurement method. Foot Ankle Surg 2016;22(4):233–8. https://doi.org/10.1016/j.fas.2015.10.002

[34] Burssens A, Barg A, van Ovost E, et al. The hind- and midfoot alignment computed after a medializing calcaneal osteotomy using a 3D weightbearing CT. Int J Comput Assist Radio Surg 2019;14(8):1439–47. https://doi.org/10.1007/s11548-019-01949-7

[35] Lintz F, Bernasconi A, Baschet L, Fernando C, Mehdi N, de Cesar Netto C. Relationship between chronic lateral ankle instability and hindfoot varus using weight-bearing cone beam computed tomography. Foot Ankle Int 2019;40(10):1175–81. https://doi.org/10.1177/1071100719858309

[36] Lintz F, Welck M, Bernasconi A, et al. 3D biometrics for hindfoot alignment using weightbearing CT. Foot Ankle Int 2017;38(6):684–9. https://doi.org/10.1177/1071100717690806

[37] de Cesar Netto C, Bernasconi A, Roberts L, et al. Foot alignment in symptomatic national basketball association players using weightbearing cone beam computed tomography. Orthop J Sports Med 2019;7(2). https://doi.org/10.1177/2325967119826081

[38] Bernasconi A, Cooper L, Lyle S, et al. Intraobserver and interobserver reliability of cone beam weightbearing semi-automatic three-dimensional measurements in symptomatic pes cavovarus. Foot Ankle Surg 2020;26(5):564–72. https://doi.org/10.1016/j.fas.2019.07.005

[39] Burssens A, Van Herzele E, Leenders T, et al. Weightbearing CT in normal hindfoot alignment — Presence of a constitutional valgus? Foot Ankle Surg 2018;24(3):213–8. https://doi.org/10.1016/j.fas.2017.02.006

[40] Patel S, Bernasconi A, Thornton J, et al. Relationship between foot posture index and weight bearing computed tomography 3D biometrics to define foot alignment. Gait Posture 2020;80:143–7. https://doi.org/10.1016/j.gaitpost.2020.05.038

[41] Day MA, Ho M, Dibbern K, et al. Correlation of 3D joint space width from weightbearing CT with outcomes after intra-articular calcaneal fracture. Foot Ankle Int 2020;41(9):1106–16. https://doi.org/10.1177/1071100720933891

[42] Fuller RM, Kim J, An TW, et al. Assessment of flatfoot deformity using digitally reconstructed radiographs: reliability and comparison to conventional radiographs. Foot Ankle Int 2022;43(7):983–93. https://doi.org/10.1177/10711007221089260

[43] Auch E, Barbachan Mansur NS, Alexandre Alves T, et al. Distal tibiofibular syndesmotic widening in progressive collapsing foot deformity. Foot Ankle Int 2021;42(6):768–75. https://doi.org/10.1177/1071100720982907

[44] Lintz F, Bernasconi A, Li S, et al. Diagnostic accuracy of measurements in progressive collapsing foot deformity using weight bearing computed tomography: a matched case-control study. Foot Ankle Surg 2022;28(7):912–8. https://doi.org/10.1016/j.fas.2021.12.012

[45] De Cesar Netto C, Godoy-Santos AL, Saito GH, et al. Subluxation of the middle facet of the subtalar joint as a marker of peritalar subluxation in adult acquired flatfoot deformity: a case-control study. J Bone Jt Surg Am Vol 2019;101(20):1838–44. https://doi.org/10.2106/JBJS.19.00073

[46] Lalevée M, Barbachan Mansur NS, Rojas EO, et al. Prevalence and pattern of lateral impingements in the progressive collapsing foot deformity. Arch Orthop Trauma Surg 2021;143(1):161–8. https://doi.org/10.1007/s00402-021-04015-7

[47] de Cesar Netto C, Saito GH, Roney A, et al. Combined weightbearing CT and MRI assessment of flexible progressive collapsing foot deformity. Foot Ankle Surg 2021;27(8):884–91. https://doi.org/10.1016/j.fas.2020.12.003

[48] Krähenbühl N, Kvarda P, Susdorf R, et al. Assessment of progressive collapsing foot deformity using semiautomated 3d measurements derived from weight-bearing CT scans. Foot Ankle Int 2022;43(3):363–70. https://doi.org/10.1177/10711007211049754

[49] Kim J, Rajan L, Fuller R, et al. Radiographic CUtoff Values for Predicting Lateral Bony Impingement in Progressive Collapsing Foot Deformity. Foot Ankle Int 2022;43(9):1219–26. https://doi.org/10.1177/10711007221099010

[50] Jeng CL, Rutherford T, Hull MG, Cerrato RA, Campbell JT. Assessment of bony subfibular impingement in flatfoot patients using weight-bearing CT scans. Foot Ankle Int 2019;40(2):152–8. doi:http://dx.doi.org/10.1177/1071100718804510.

[51] de Cesar Netto C, Silva T, Li S, et al. Assessment of posterior and middle facet subluxation of the subtalar joint in progressive flatfoot deformity. Foot Ankle Int 2020;41(10):1190–7. https://doi.org/10.1177/1071100720936603

[52] de Cesar Netto C, Shakoor D, Roberts L, et al. Hindfoot alignment of adult acquired flatfoot deformity: A comparison of clinical assessment and weight-bearing cone beam CT examinations. Foot Ankle Surg V 2019;25(6):790–7. https://doi.org/10.1016/j.fas.2018.10.008

[53] Shakoor D, de Cesar Netto C, Thawait GK, et al. Weight-bearing radiographs and cone-beam computed tomography examinations in adult acquired flatfoot deformity. Foot Ankle Surg 2021;27(2):201–6. https://doi.org/10.1016/j.fas.2020.04.011

[54] de Cesar Netto C, Bang K, Mansur NS, et al. Multiplanar semiautomatic assessment of foot and ankle offset in adult acquired flatfoot deformity. Foot Ankle Int 2020;41(7):839–48. https://doi.org/10.1177/1071100720920274

[55] Day J, de Cesar Netto C, Nishikawa DRC, et al. Three-dimensional biometric weightbearing CT evaluation of the operative treatment of adult-acquired flatfoot deformity. Foot Ankle Int 2020;41(8):930–6. https://doi.org/10.1177/1071100720925423

[56] Behrens A, Dibbern K, Lalevée M, et al. Coverage maps demonstrate 3D Chopart joint subluxation in weightbearing CT of progressive collapsing foot deformity. Sci Rep 2022;12(1). https://doi.org/10.1038/s41598-022-23638-3

[57] Dibbern KN, Li S, Vivtcharenko V, et al. Three-dimensional distance and coverage maps in the assessment of peritalar subluxation in progressive collapsing foot deformity. Foot Ankle Int 2021;42(6):757–67. https://doi.org/10.1177/1071100720983227

[58] Netto CDC, Schon LC, Thawait GK, et al. Flexible adult acquired flatfoot deformity: comparison between weight-bearing and non-weight-bearing measurements using cone-beam computed tomography. J Bone Jt Surg Am 2017;99(18):e98. https://doi.org/10.2106/JBJS.16.01366

[59] Ortolani M, Leardini A, Pavani C, et al. Angular and linear measurements of adult flexible flatfoot via weight-bearing CT scans and 3D bone reconstruction tools. Sci Rep 2021;11(1):16139. https://doi.org/10.1038/s41598-021-95708-x

[60] Richter M, Lintz F, Zech S, Meissner SA. Combination of PedCAT weightbearing CT with pedography assessment of the relationship between anatomy-based foot center and force/pressure-based center of gravity. Foot Ankle Int 2018;39(3):361–8. https://doi.org/10.1177/1071100717744206

[61] Richter M, Zech S, Hahn S, Naef I, Merschin D. Combination of pedCAT® for 3D imaging in standing position with pedography shows no statistical correlation of bone position with force/pressure distribution. J Foot Ankle Surg 2016;55(2):240–6. https://doi.org/10.1053/j.jfas.2015.10.004

[62] Michalski MP, An TW, Haupt ET, Yeshoua B, Salo J, Pfeffer G. Abnormal bone morphology in charcot-marie-tooth disease. Foot Ankle Int 2022;43(4):576–81. https://doi.org/10.1177/10711007211055460

[63] An T, Haupt E, Michalski M, Salo J, Pfeffer G. Cavovarus with a twist: midfoot coronal and axial plane rotational deformity in charcot-marie-tooth disease. Foot Ankle Int 2022;43(5):676–82. https://doi.org/10.1177/10711007211064600

[64] Sangoi D, Ranjit S, Bernasconi A, et al. 2D manual vs 3D automated assessment of alignment in normal and charcot-marie-tooth cavovarus feet using weight-bearing CT. Foot Ankle Int 2022;43(7):973–82. https://doi.org/10.1177/10711007221084308

[65] Sripanich Y, Weinberg MW, Krähenbühl N, Rungprai C, Saltzman CL, Barg A. Reliability of measurements assessing the Lisfranc joint using weightbearing computed tomography imaging. Arch Orthop Trauma Surg 2021;141(5):775–81. https://doi.org/10.1007/s00402-020-03477-5

[66] Falcon S, McCormack T, Mackay M, et al. Retrospective chart review: weight-bearing CT scans and the measurement of the Lisfranc ligamentous complex. Foot Ankle Surg 2023;29(1):39–43. https://doi.org/10.1016/j.fas.2022.08.011

[67] Bhimani R, Sornsakrin P, Ashkani-Esfahani S, et al. Using area and volume measurement via weightbearing CT to detect Lisfranc instability. J Orthop Res 2021;39(11):2497–505. https://doi.org/10.1002/jor.24970

[68] Steadman J, Sripanich Y, Rungprai C, Mills MK, Saltzman CL, Barg A. Comparative assessment of midfoot osteoarthritis diagnostic sensitivity using weightbearing computed tomography vs weightbearing plain radiography. Eur J Radio 2021;134:109419. https://doi.org/10.1016/j.ejrad.2020.109419

[69] Mansur NSB, Lalevee M, Schmidt E, et al. Correlation between indirect radiographic parameters of first metatarsal rotation in hallux valgus and values on weight-bearing computed tomography. Int Orthop 2021;45(12):3111–8. https://doi.org/10.1007/s00264-021-05136-9

[70] Zhong Z, Zhang P, Duan H, Yang H, Li Q, He F. A comparison between X-ray imaging and an innovative computer-aided design method based on weight-bearing CT scan images for assessing Hallux Valgus. J Foot Ankle Surg 2021;60(1):6–10. https://doi.org/10.1053/j.jfas.2018.12.044

[71] Lalevée M, Barbachan Mansur NS, Lee HY, et al. Distal metatarsal articular angle in hallux valgus deformity. fact or fiction? a 3-dimensional weightbearing CT assessment. Foot Ankle Int 2022;43(4):495–503. https://doi.org/10.1177/10711007211051642
[72] Najefi AA, Katmeh R, Zaveri AK, et al. Imaging findings and first metatarsal rotation in hallux valgus. Foot Ankle Int 2022;43(5):665–75. https://doi.org/10.1177/10711007211064609
[73] Clarke AJ, Conti SF, Conti M, Fadle AA, Ellis SJ, Miller MC. The association of crista volume with sesamoid position as measured from 3D reconstructions of weightbearing CT scans. Foot Ankle Int 2022;43(5):658–64. https://doi.org/10.1177/10711007211061363
[74] Mahmoud K, Metikala S, Mehta SD, Fryhofer GW, Farber DC, Prat D. The role of weightbearing computed tomography scan in hallux valgus. Foot Ankle Int 2021;42(3):287–93. https://doi.org/10.1177/1071100720962398
[75] Lee HY, Mansur NS, Lalevee M, et al. Does metatarsus primus elevatus exist in hallux rigidus? A weightbearing CT case–control study. Arch Orthop Trauma Surg 2021;143(2):755–61. https://doi.org/10.1007/s00402-021-04168-5
[76] de Carvalho KAM, Walt JS, Ehret A, et al. Comparison between weightbearing-CT semiautomatic and manual measurements in Hallux Valgus. Foot Ankle Surg 2022;28(4):518–25. https://doi.org/10.1016/j.fas.2022.02.014
[77] Day J, de Cesar Netto C, Richter M, et al. Evaluation of a weightbearing CT artificial intelligence-based automatic measurement for the m1-m2 intermetatarsal angle in hallux valgus. Foot Ankle Int 2021;42(11):1502–9. https://doi.org/10.1177/10711007211015177
[78] Conti MS, Patel TJ, Caolo KC, et al. Correlation of different methods of measuring pronation of the first metatarsal on weightbearing CT scans. Foot Ankle Int 2021;42(8):1049–59. https://doi.org/10.1177/10711007211003090
[79] Conti MS, MacMahon A, Ellis SJ, Cody EA. Effect of the modified lapidus procedure for hallux valgus on foot width. Foot Ankle Int 2020;41(2):154–9. https://doi.org/10.1177/1071100719884556
[80] Conti MS, Willett JF, Garfinkel JH, et al. Effect of the modified lapidus procedure on pronation of the first ray in hallux valgus. Foot Ankle Int 2020;41(2):125–32. https://doi.org/10.1177/1071100719883325
[81] Carvalho KAM, de, Mallavarapu V, Ehret A, et al. The Use of Advanced Semiautomated Bone Segmentation in Hallux Rigidus. Foot Ankle Orthop 2022;7(4). https://doi.org/10.1177/24730114221137597
[82] Welck MJ, Singh D, Cullen N, Goldberg A. Evaluation of the 1st metatarso-sesamoid joint using standing CT - The Stanmore classification. Foot Ankle Surg 2018;24(4):314–9. https://doi.org/10.1016/j.fas.2017.03.005
[83] Belvedere C, Giacomozzi C, Carrara C, et al. Correlations between weight-bearing 3D bone architecture and dynamic plantar pressure measurements in the diabetic foot. J Foot Ankle Res 2020;13(1):64. https://doi.org/10.1186/s13047-020-00431-x
[84] Richter M, Seidl B, Zech S, Hahn S. PedCAT for 3D-imaging in standing position allows for more accurate bone position (angle) measurement than radiographs or CT. Foot Ankle Surg 2014;20(3):201–7. https://doi.org/10.1016/j.fas.2014.04.004
[85] Richter M, Lintz F, de Cesar Netto C, Barg A, Burssens A. Results of more than 11,000 scans with weightbearing CT — Impact on costs, radiation exposure, and procedure time. Foot Ankle Surg 2020;26(5):518–22. https://doi.org/10.1016/j.fas.2019.05.019
[86] Richter M, Duerr F, Schilke R, Zech S, Meissner SA, Naef I. Semi-automatic software-based 3D-angular measurement for Weight-Bearing CT (WBCT) in the foot provides different angles than measurement by hand. Foot Ankle Surg 2022;28(7):919–27. https://doi.org/10.1016/j.fas.2022.01.001
[87] Richter M, Schilke R, Duerr F, Zech S, Andreas Meissner S, Naef I. Automatic software-based 3D-angular measurement for Weight-Bearing CT (WBCT) provides different angles than measurement by hand. Foot Ankle Surg 2022;28(7):863–71. https://doi.org/10.1016/j.fas.2021.11.010
[88] Slim K, Nini E, Forestier D, Kwiatkowski F, Panis Y, Chipponi J. Methodological index for non-randomized studies (Minors): Development and validation of a new instrument. ANZ J Surg 2003;73(9):712–6. https://doi.org/10.1046/j.1445-2197.2003.02748.x
[89] Ekhtiari S, Horner NS, Bedi A, Ayeni OR, Khan M. The learning curve for the latarjet procedure: a systematic review. Orthop J Sports Med 2018;6(7). https://doi.org/10.1177/2325967118786930
[90] Lintz F, Mast J, Bernasconi A, Mehdi N, de Cesar Netto C, Fernando C. Weightbearing topographical study of periprosthetic cysts and alignment in total ankle replacement. Foot Ankle Int 2020;41(1):1–9. https://doi.org/10.1177/1071100719891411
[91] Kvarda P, Krähenbühl N, Susdorf R, Burssens A, Ruiz R, Barg A. High reliability for semiautomated 3d measurements based on weightbearing CT scans. Foot Ankle Int 2022;43(1):91–5. https://doi.org/10.1177/10711007211034522
[92] Barg A, Bailey T, Richter M, de Cesar Netto C, Lintz F, Burssens A, Phisitkul P, Hanrahan CJ, Saltzman CL. Weightbearing computed tomography of the foot and ankle: emerging technology topical review. Foot Ankle Int 2018;39(3):376–86. https://doi.org/10.1177/1071100717740330
[93] Richter M, de Cesar Netto C, Lintz F, Barg A, Burssens A, Ellis S. The assessment of ankle osteoarthritis with weight-bearing computed tomography. Foot Ankle Clin 2022;27(1):13–36. https://doi.org/10.1016/j.fcl.2021.11.001
[94] Peiffer M, Dhont T, Cuigniez F, et al. Application of external torque enhances the detection of subtle syndesmotic ankle instability in a weight-bearing CT. (Online ahead of print). Knee Surg Sports Trauma Arthrosc2023. https://doi.org/10.1007/s00167-023-07536-3